Experiments in Fluid Mechanics ExFM 2017

Multiscale Modal Analysis of Experimental and Numerical Data

Miguel. A. Mendez[1*] , Mikhael Balabane[2], Jean-Marie Buchlin[1]

[1]von Karman Institute for Fluid Dynamics, Rhode-St-Genèse, Belgium

[2]Laboratoire Analyse Geometrie et Applications, Paris 13, France

Warsaw, Poland, 23-24 October, 2017

von KARMAN INSTITUTE FOR FLUID DYNAMICS

ULB UNIVERSITÉ LIBRE DE BRUXELLES

Table of Contents

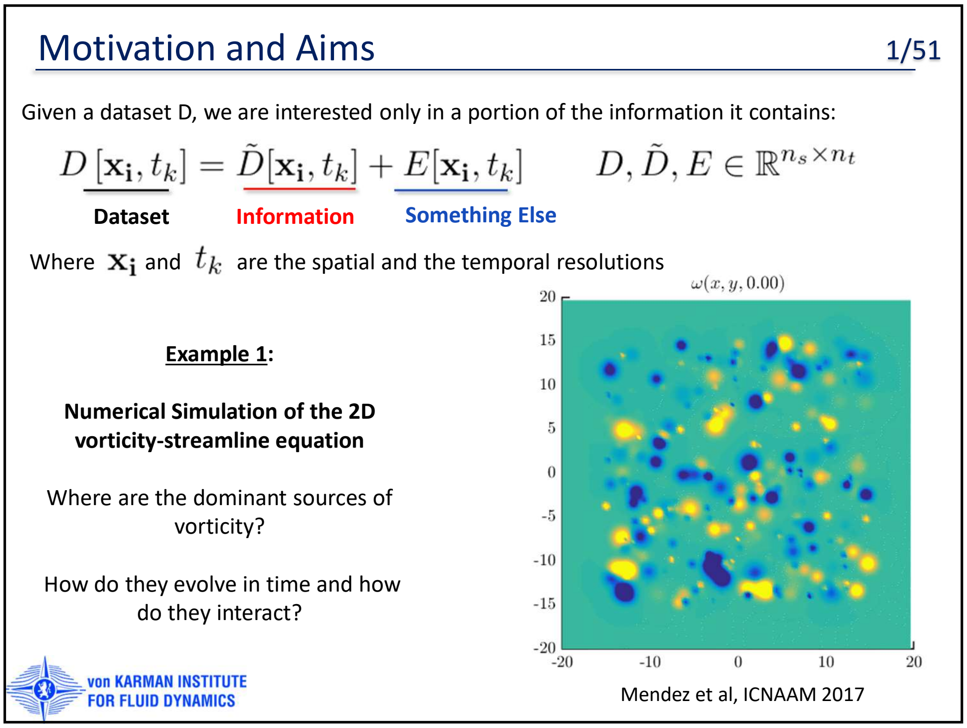

Motivation and Aims

Given a dataset D, we are interested only in a portion of the information it contains:

$$\underbrace{D\,[\mathbf{x_i}, t_k]}_{\text{Dataset}} = \underbrace{\tilde{D}[\mathbf{x_i}, t_k]}_{\text{Information}} + \underbrace{E[\mathbf{x_i}, t_k]}_{\text{Something Else}} \qquad D, \tilde{D}, E \in \mathbb{R}^{n_s \times n_t}$$

Where $\mathbf{x_i}$ and t_k are the spatial and the temporal resolutions

Example 1:

Numerical Simulation of the 2D vorticity-streamline equation

Where are the dominant sources of vorticity?

How do they evolve in time and how do they interact?

Mendez et al, ICNAAM 2017

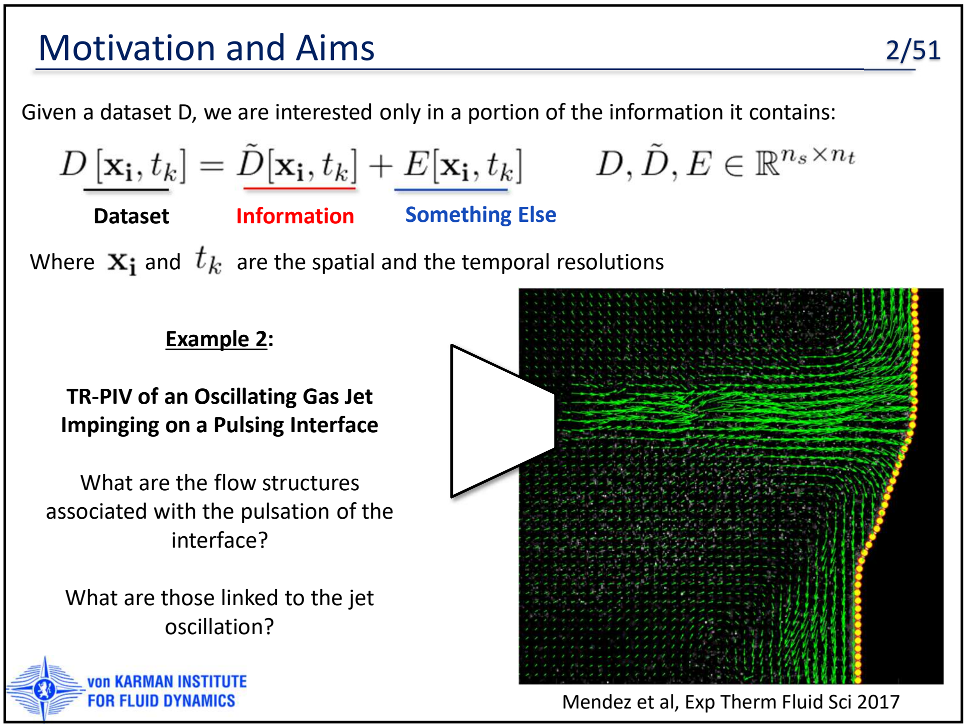

Motivation and Aims

Given a dataset D, we are interested only in a portion of the information it contains:

$$\underbrace{D\,[\mathbf{x_i}, t_k]}_{\text{Dataset}} = \underbrace{\tilde{D}[\mathbf{x_i}, t_k]}_{\text{Information}} + \underbrace{E[\mathbf{x_i}, t_k]}_{\text{Something Else}} \qquad D, \tilde{D}, E \in \mathbb{R}^{n_s \times n_t}$$

Where $\mathbf{x_i}$ and t_k are the spatial and the temporal resolutions

Example 2:

TR-PIV of an Oscillating Gas Jet Impinging on a Pulsing Interface

What are the flow structures associated with the pulsation of the interface?

What are those linked to the jet oscillation?

Mendez et al, Exp Therm Fluid Sci 2017

What is a Decomposition ?

Decomposing means ‘to break down’ into constituent simpler parts, e.g.:

$$\underline{D\left[\mathbf{x_i},t_k\right]} = \underline{D_1[\mathbf{x_i},t_k] + D_2[\mathbf{x_i},t_k]} + \underline{D_3[\mathbf{x_i},t_k]\cdots + D_r[\mathbf{x_i},t_k]}$$

Dataset **Information** **Something Else**

Each of part has its own spatial and temporal evolution, and it is referred to as **mode.**

We search for modes that can be written in a variable separated and normalized form:

Spatial structure Energy Contribution

$$D\left[\mathbf{x_i},t_k\right] = \sum_{r=1}^{n_t} \underline{S_r\left[\mathbf{x_i}\right]}\,\underline{T_r[t_k]} = \sum_{r=1}^{n_t} \sigma_r \underline{\phi_r\left[\mathbf{x_i}\right]\psi_r[t_k]}$$

Temporal Evolution Unitary energy structures/evolutions

The most common decomposition is the Time-Discrete Fourier Transform (TDFT) where the temporal evolution of each mode is assumed to be harmonic:

$$\psi_n[k] = e^{-2\pi \mathrm{i}\frac{(k-1)(n-1)}{n_t}} \quad \text{with} \quad k = \frac{t_k - 1}{\Delta t} \quad \text{and} \quad n \in \left[-\frac{n}{2}, \frac{n}{2} - 1\right]$$

In order to have a frequency span $f_n = \left[-\frac{f_s}{2}, \frac{f_s}{2}\right]$

von KARMAN INSTITUTE FOR FLUID DYNAMICS

Table of Contents

The Algebra of any Decomposition

It is now useful to see a discrete decomposition from an algebraic point of view.
At the scope assume we organize each snapshot into a column vector and we do the same for the spatial and the temporal structure of each mode:

$$D\,[\mathbf{i},k] = \begin{bmatrix} d_1[\mathbf{x_i}] & d_2[\mathbf{x_i}] & \dots & d_k[\mathbf{x_i}] \\ \vdots & \vdots & \vdots & \vdots \end{bmatrix}$$ Data Matrix $\in \mathbb{R}^{n_s \times n_t}$

$$\Phi\,[\mathbf{i},r] = \begin{bmatrix} \phi_1[\mathbf{x_i}] & \phi_2[\mathbf{x_i}] & \dots & \phi_n[\mathbf{x_i}] \\ \vdots & \vdots & \vdots & \vdots \end{bmatrix}$$ Spatial Structures $\in \mathbb{C}^{n_s \times r}$

Energy Contribution $\in \mathbb{R}^{r \times r}$ $$\Sigma\,[r,r] = \begin{bmatrix} \sigma_1 & \dots & 0 \\ \vdots & \ddots & \vdots \\ 0 & \dots & \sigma_r \end{bmatrix}$$

Temporal Evolutions $\in \mathbb{C}^{n_t \times r}$ $$\Psi\,[k,r] = \begin{bmatrix} \psi_1[k] & \psi_2[k] & \dots & \psi_n[k] \\ \vdots & \vdots & \vdots & \vdots \end{bmatrix}$$

The Algebra of any Decomposition

All the decomposition will therefore be written via matrix multiplication:

$$D[\mathbf{x}_i, t_k] = \sum_{r=1}^{n_t} \sigma_r\, \phi_r[\mathbf{x}_i]\, \psi_r[t_k] = \Phi\, \Sigma\, \Psi^* \qquad \text{Eq 1}$$

To close the problem, one must set constraints in the spatial or in the temporal bases.

Pre-Defined (Supervised)

Analytical (Eigen-Functions)

Fourier exponentials
Legendre Polynomials
Chebyshev Polynomials
Bessel Functions

'ad hoc'

Fourier exponentials
Wavelets

Inferred (Unsupervised)

Proper Orthogonal Decomposition (POD)

Dynamic Mode Decomposition (DMD)

Spectral Proper Orthogonal Decomposition (SPOD)

The fundamental Classes

$$D[\mathbf{x}_i, t_k] = \sum_{r=1}^{n_t} \sigma_r \, \phi_r[\mathbf{x}_i] \, \psi_r[t_k] = \Phi \, \Sigma \, \Psi^*$$

Eq 1

Energy Based: POD	Frequency Based: DMD	Mixed: SPOD
(Lumley,1967)	**(Schmidt, Rowley, 2009)**	(M Sieber**, 2015)**
Goal: **Minimize the number of mode required**	**Goal:** **Harmonic Modes**	**Goal:** **Mixing 1 and 2**
☑ Advantage: Energy Optimality	☑ Advantage: Spectral separation	☑ Advantage: Good blending between POD/DFT
☒ Pitfalls: Possible Spectral Mixing	☒ Pitfalls: Poor convergence, possible finite blow-ups	☒ Pitfalls: Possible poor convergence and lost of data inference

---

The fundamental Classes: POD

$$D[\mathbf{x}_i, t_k] = \sum_{r=1}^{n_t} \sigma_r \, \phi_r[\mathbf{x}_i] \, \psi_r[t_k] = \Phi \, \Sigma \, \Psi^*$$

Eq 1

Energy Based: POD

We assume that both spatial and temporal dependencies form an orthonormal set.

For a real dataset, orthonormality reads

$$\Phi^T \Phi = \Psi^T \Psi = I$$

Therefore these bases are the set of eigenvectors of the covariance matrices, and the associated energies are the square roots of the corresponding eigenvectors

$$K = D^T D = \Psi \Sigma \Big(\Phi^T \Phi \Big) \Sigma \Psi^T = \Psi \Sigma^2 \Psi^T$$

$$C = D D^T = \Phi \Sigma \Big(\Psi^T \Psi \Big) \Sigma \Phi^T = \Phi \Sigma^2 \Phi^T$$

The POD decomposition in Eq 1 becomes simply the Singular Value Decomposition (SVD) of the dataset D. The energy optimality is guaranteed by the Eckart-Young theorem.

PROBLEM: Eigenvectors are unique up to repeated singular values

The fundamental Classes: DFT/DMD

$$D[\mathbf{x}_i, t_k] = \sum_{r=1}^{n_t} \sigma_r \, \phi_r[\mathbf{x}_i] \, \psi_r[t_k] = \Phi \, \Sigma \, \Psi^* \qquad \text{Eq 1}$$

Frequency Based: DMD

As for the DFT, the DMD the temporal basis has a Vandermonde form:

$$\Psi = \frac{1}{\sqrt{n_t}} \begin{bmatrix} 1 & 1 & 1 & \dots & 1 \\ 1 & w & w^2 & \dots & w^{(r-1)} \\ \vdots & \vdots & \ddots & \vdots & \\ 1 & w^{n_t-1} & w^{2(n_t-1)} & \dots & w^{(r-1)(n_t-1)} \end{bmatrix}$$

$$\Psi^H \Psi = I$$

$$X = \Phi \Sigma \Psi^H$$

$$\hookrightarrow X \, \Psi = \Phi \Sigma$$

DFT: $\Psi = F$

powers of a real, fundamental frequency

$$f_0 = 1/T = n_t/\Delta t$$

$$w = \exp\Big(\mathrm{i}\,2\pi f_0 \Delta t\Big) = \exp\Big(\frac{2\pi \mathrm{i}}{n_t}\Big)$$

DMD: $\Psi = Z$

Complex frequencies of the system

$$w_i = \exp\Big(\mathrm{i}\,\omega_i \Delta t\Big)$$

with

$$i \in [1, r-1] \qquad \omega_i \in \mathbb{C}$$

The fundamental Classes: DFT/DMD

$$D[\mathbf{x}_i, t_k] = \sum_{r=1}^{n_t} \sigma_r \, \phi_r[\mathbf{x}_i] \, \psi_r[t_k] = \Phi \, \Sigma \, \Psi^* \qquad \text{Eq 1}$$

Frequency Based: DMD

The DMD assumes that it is possible to describe the data as a linear dynamical system, then each realization can be obtained from the previous via matrix multiplication with a propagator:

$$d_{k+1} = P d_k = P^k d_1 = \Phi \Lambda^k \Phi^{-1} d_1$$

With the complex eigenvalues controlling the evolution of each mode

$$\lambda_i = \exp(\mathrm{i}\omega_i) \rightarrow \lambda_i^k = \exp\left(\mathrm{i}\omega_i \frac{t_k}{\Delta t}\right)$$

DMD aims at building an approximated propagator from the dataset.
Note: provided that the imaginary part of the frequency is zero, DMD converges towards a DFT (See Mezic *et al* 2005, Rowley *et al* 2009, Chen *et al* 2012)

The fundamental Classes: DFT/DMD

$$D[\mathbf{x}_i, t_k] = \sum_{r=1}^{n_t} \sigma_r\, \phi_r[\mathbf{x}_i]\, \psi_r[t_k] = \Phi\,\Sigma\,\Psi^*$$

Eq 1

Frequency Based: DFT/DMD

The standard algorithm (Schmid, 2010) is organized in three steps:

1) Rearrange the dataset introducing P

$$D_{1,n_t-1} = D[d_1, \dots d_{n_t-1}] \qquad D_{2,n_t} = D[d_2, \dots d_{n_t}] \longrightarrow D_{2,n_t} = P D_{1,n_t-1}$$

2) Project P onto the POD modes of the dataset to obtained an approximate P

$$D_{2,n_t} = P\,U\,S\,V^T \longrightarrow U^T D_{2,n_t} V S^{-1} = U^T P\,U = \tilde{P}$$

3) Compute the eigenfrequencies from the approximated P

$$\tilde{P} = Q\,\Lambda Q^{-1} \longrightarrow \Phi = U\,Q$$

Given the spatial structures and the temporal modes, the amplitudes can be easily recovered (see Schmid, 2010)

PROBLEM(s)

At best (DMD approaching DFT), the convergence is poor.
At worst (bad conditioning of P), the DMD does not converge

The fundamental Classes: SPOD

$$D[\mathbf{x}_i, t_k] = \sum_{r=1}^{n_t} \sigma_r\, \phi_r[\mathbf{x}_i]\, \psi_r[t_k] = \Phi\,\Sigma\,\Psi^*$$

Eq 1

Mixed: SPOD

The SPOD (Sieber, 2016) modifies the eigenvalue problem in the computation of the POD by filtering the covariance matrix along the diagonals.
The idea is that harmonic modes in the POD arise when the covariance matrix K is close to a Toepliz Circulant Matrix.

$K = D^T D$

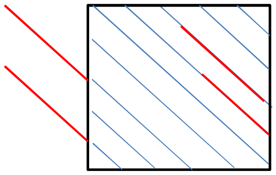

The 1D low pass filter acting
Along the diagonals forces this covariance pattern

filter's impulse response

$$\tilde{K}_{i,j} = \sum_{l=-n_F}^{n_F} \underline{f_l} K_{i,j}$$

Then, the algorithm is a standard POD:

$$\tilde{K} = \Psi \Sigma^2 \Psi^{-1} \longrightarrow \Phi = D\,\Psi\,\Sigma^{-1}$$

PROBLEM(s)

Invasive treatment of the correlation matrix and loss of orthogonality: who is the new K? what is the good filter strength?

Table of Contents

Synthetic Test of the POD Limit

$$D(x,t)=\sum_{i=1}^{2}A_i\,\exp\left(\frac{(\mathbf{x}-\mathbf{x_{i0}})^2}{2\sigma^2}\right)T_i(t)$$

$$\Delta x=0.15 \qquad \Delta t=0.01$$

$$D\in\mathbb{R}^{(256\times256)\times512}$$

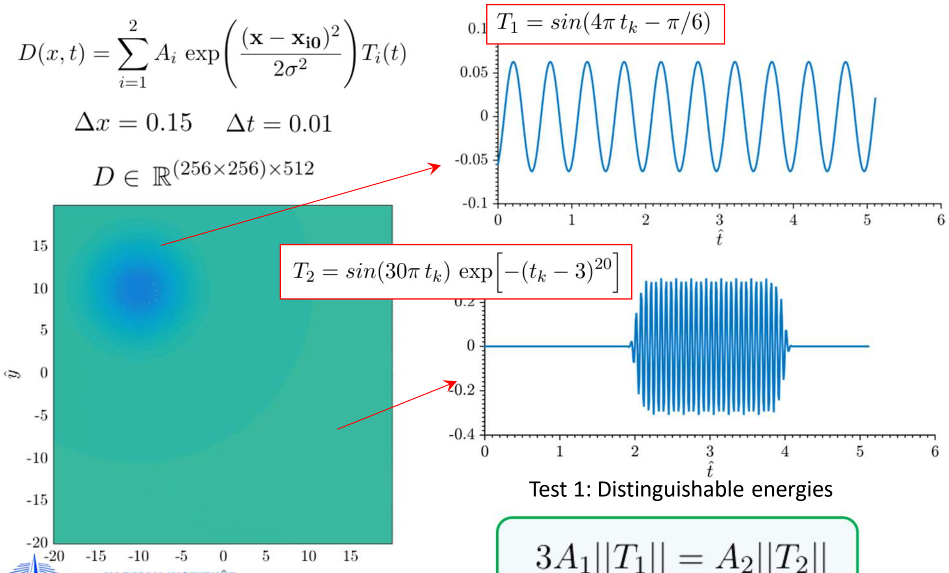

$T_1=sin(4\pi\,t_k-\pi/6)$

$T_2=sin(30\pi\,t_k)\,\exp\left[-(t_k-3)^{20}\right]$

Test 1: Distinguishable energies

$$\boxed{3A_1||T_1||=A_2||T_2||}$$

von KARMAN INSTITUTE FOR FLUID DYNAMICS

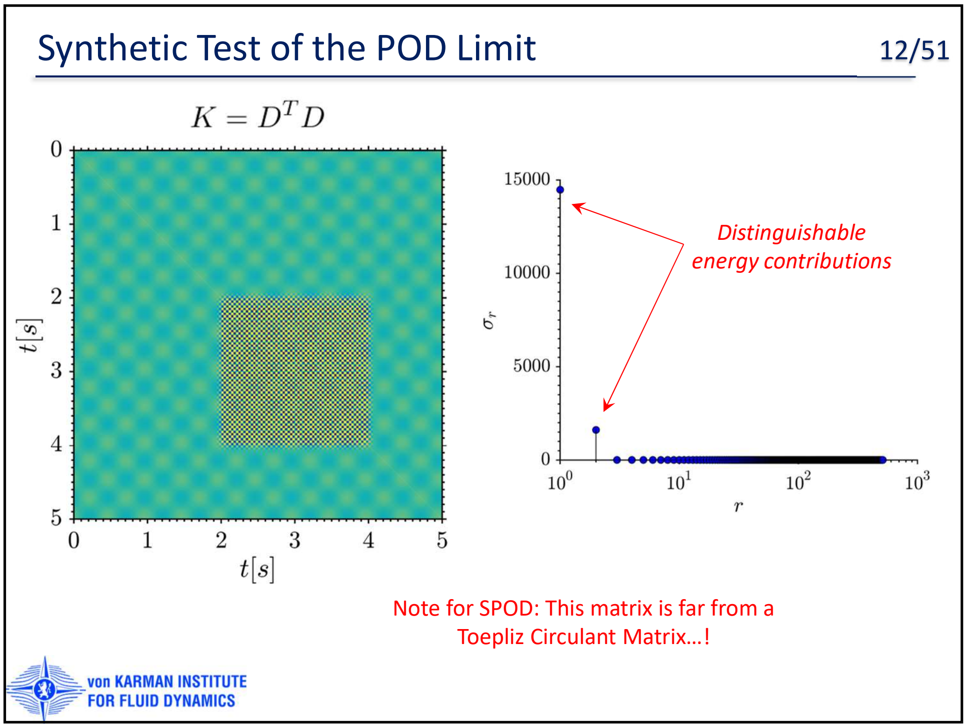

Synthetic Test of the POD Limit

12/51

$K = D^T D$

Distinguishable energy contributions

Note for SPOD: This matrix is far from a Toepliz Circulant Matrix…!

von KARMAN INSTITUTE FOR FLUID DYNAMICS

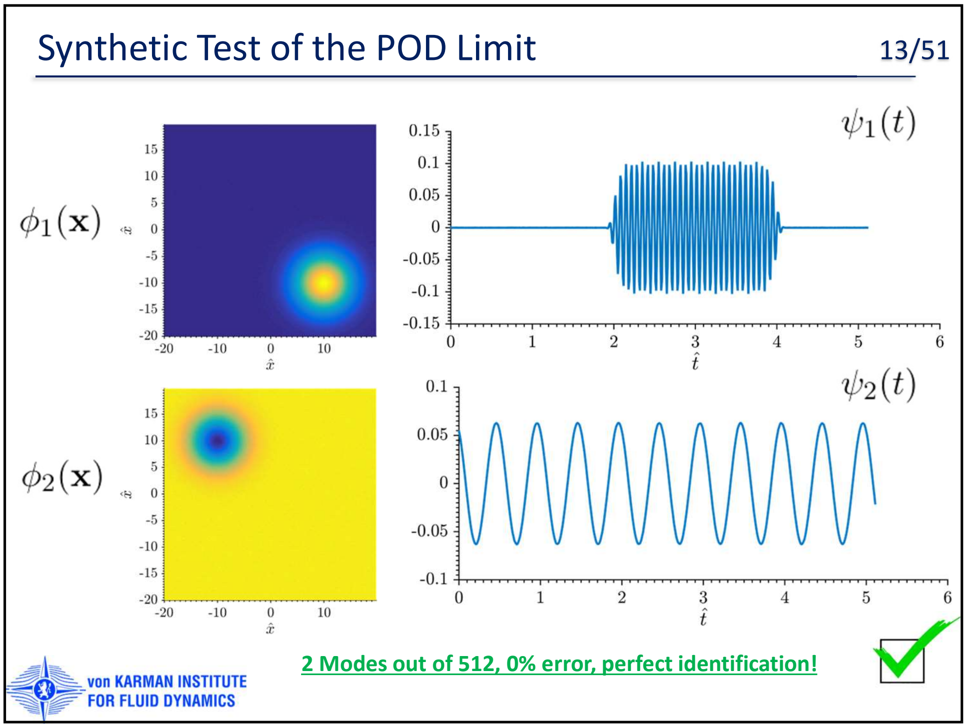

Synthetic Test of the POD Limit

13/51

$\phi_1(\mathbf{x})$

$\psi_1(t)$

$\phi_2(\mathbf{x})$

$\psi_2(t)$

2 Modes out of 512, 0% error, perfect identification! ☑

von KARMAN INSTITUTE FOR FLUID DYNAMICS

Synthetic Test of the POD Limit

$$D(x,t) = \sum_{i=1}^{2} A_i \exp\left(\frac{(\mathbf{x}-\mathbf{x_{i0}})^2}{2\sigma^2}\right) T_i(t)$$

$$\Delta x = 0.15 \qquad \Delta t = 0.01$$

$$D \in \mathbb{R}^{(256\times256)\times512}$$

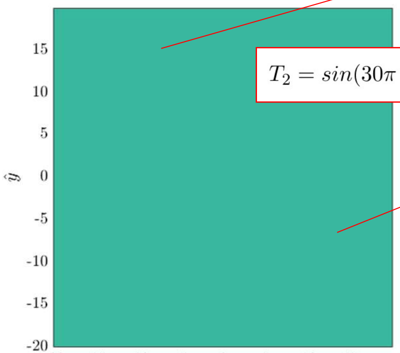

$T_1 = sin(4\pi\, t_k)$

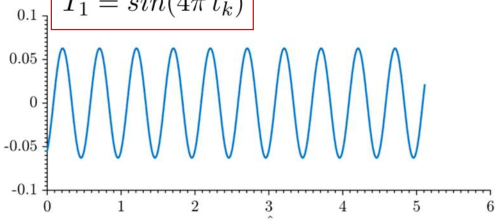

$T_2 = sin(30\pi\, t_k)\ \exp\left[-(t_k-3)^{20}\right]$

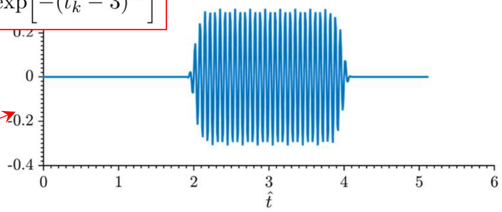

Test 2: Equal energies

$$A_1||T_1|| = A_2||T_2||$$

Synthetic Test of the POD Limit

$K = D^T D$

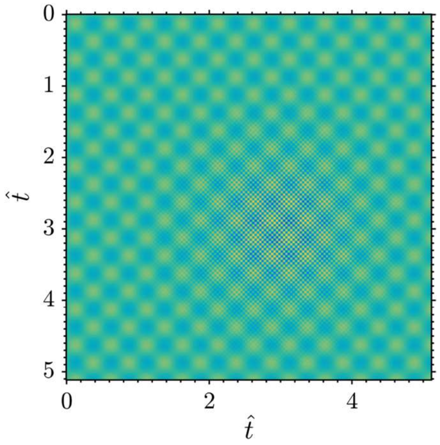

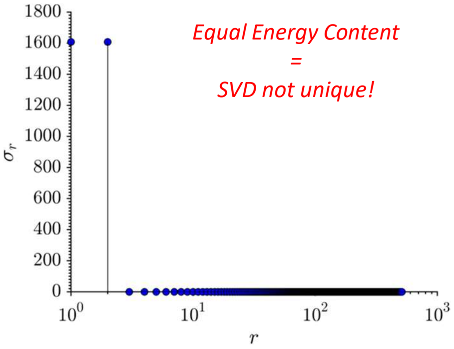

Equal Energy Content

=

SVD not unique!

We still have perfect reconstruction, but…

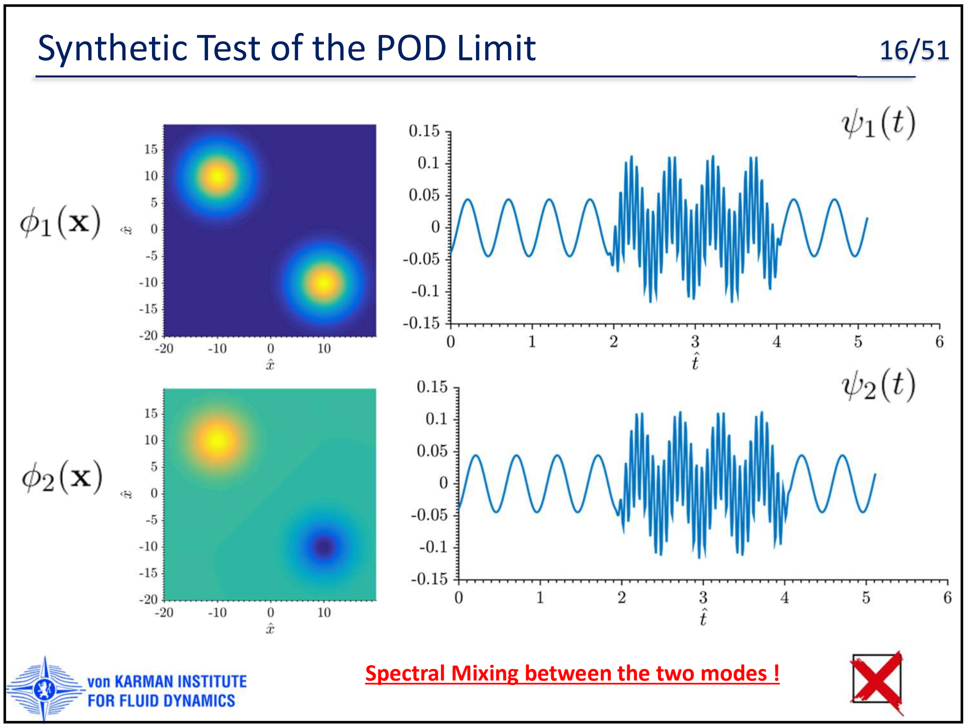

Synthetic Test of the POD Limit

Spectral Mixing between the two modes !

von KARMAN INSTITUTE
FOR FLUID DYNAMICS

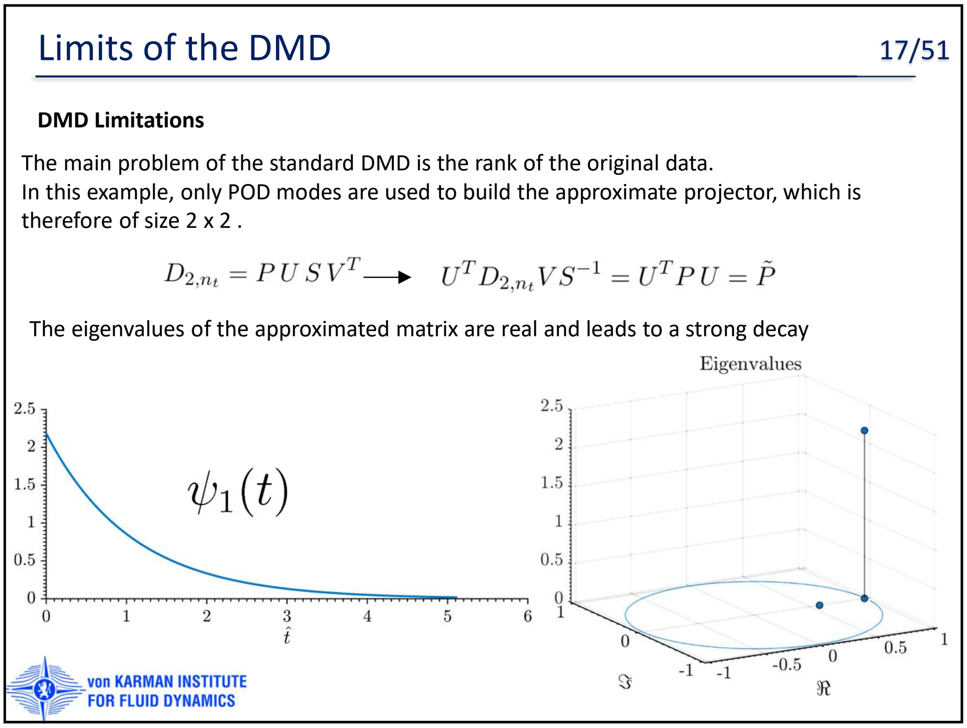

Limits of the DMD

DMD Limitations

The main problem of the standard DMD is the rank of the original data.
In this example, only POD modes are used to build the approximate projector, which is therefore of size 2 x 2 .

$$D_{2,n_t} = P\,U\,S\,V^T \longrightarrow U^T D_{2,n_t} V S^{-1} = U^T P U = \tilde{P}$$

The eigenvalues of the approximated matrix are real and leads to a strong decay

von KARMAN INSTITUTE
FOR FLUID DYNAMICS

Limits of the DMD

DMD Limitations

The main problem of the standard DMD is the rank of the original data.
In this example, only POD modes are used to build the approximate projector, which is therefore of size 2 x 2 .

$$D_{2,n_t} = P\,U\,S\,V^T \longrightarrow U^T D_{2,n_t} V S^{-1} = U^T P\,U = \tilde{P}$$

The eigenvalues of the approximated matrix are real and leads to a strong decay

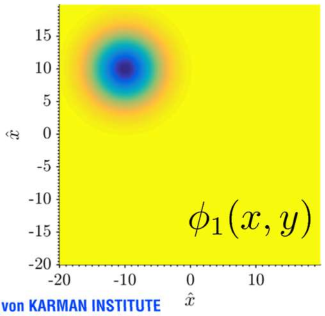

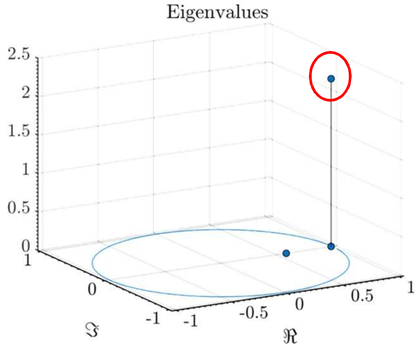

Limits of the SPOD

We consider two different sizes of the low pass filter along the diagonals

Increasing the filter side forces the covariance matrix towards a Toepliz matrix: the decomposition approaches the DFT (and inherits its problems!).

Obs: that the modes comes automatically paired

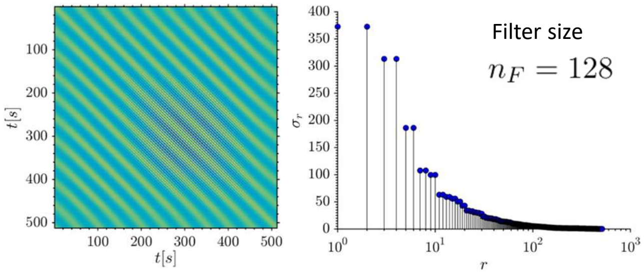

Filter size

$n_F = 128$

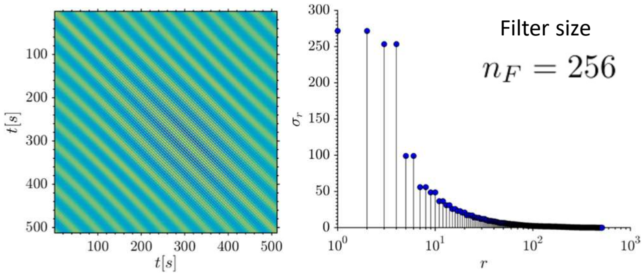

Filter size

$n_F = 256$

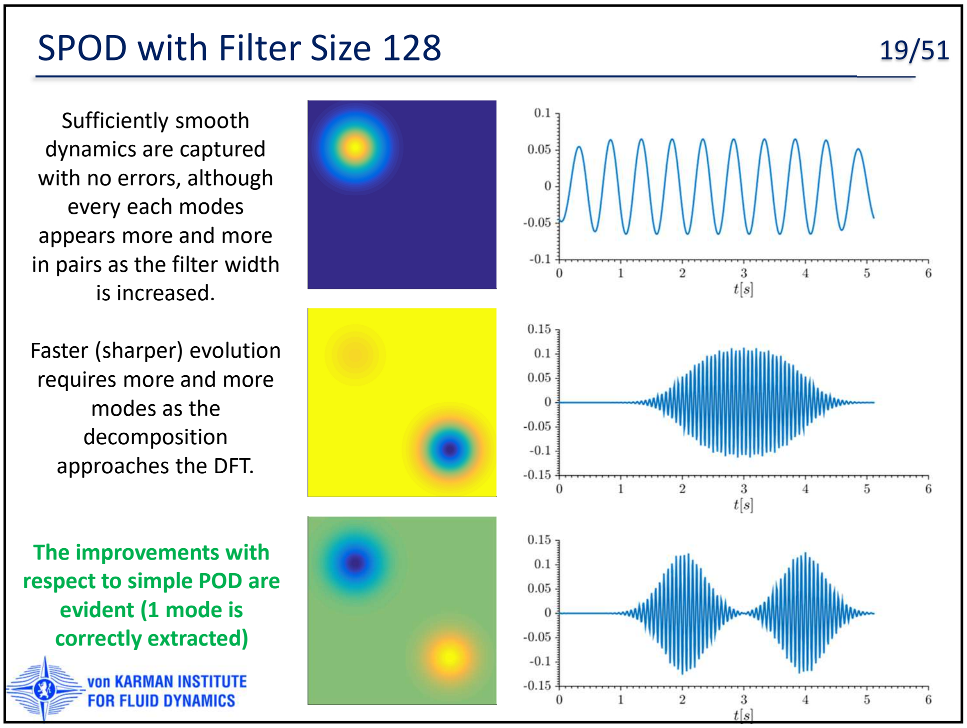

SPOD with Filter Size 128

Sufficiently smooth dynamics are captured with no errors, although every each modes appears more and more in pairs as the filter width is increased.

Faster (sharper) evolution requires more and more modes as the decomposition approaches the DFT.

The improvements with respect to simple POD are evident (1 mode is correctly extracted)

von KARMAN INSTITUTE
FOR FLUID DYNAMICS

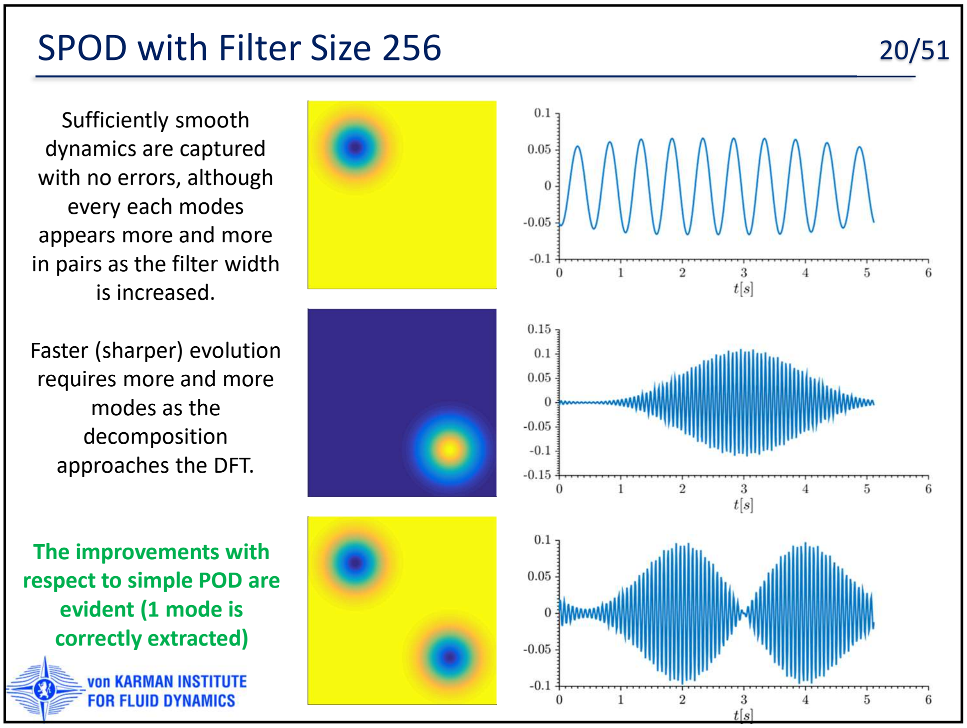

SPOD with Filter Size 256

Sufficiently smooth dynamics are captured with no errors, although every each modes appears more and more in pairs as the filter width is increased.

Faster (sharper) evolution requires more and more modes as the decomposition approaches the DFT.

The improvements with respect to simple POD are evident (1 mode is correctly extracted)

von KARMAN INSTITUTE
FOR FLUID DYNAMICS

Table of Contents

A new Decomposition: Motivation

$$D[\mathbf{x}_i, t_k] = \sum_{r=1}^{n_t} \sigma_r\, \phi_r[\mathbf{x}_i]\, \psi_r[t_k] = \Phi\, \Sigma\, \Psi^*$$

Energy Based: POD

✓

Orthogonality of the temporal modes, to be linked to K

Frequency Based: DFT/DMD

✓

Limit Frequency Bandwith but not necessarely harmonics. Avoid at any step operations in the Fourier Domain

Mixed: SPOD

✓

Use filters on K, but allow for perfect reconstruction of K.

↓

The multiscale Proper Orthogonal Decomposition (mPOD)

Table of Contents

Filtering and Eigenvector's Spectra

It is convenient to consider the spectra of a vector (1D) as the projection onto the Fourier Basis, thus as a matrix multiplication

$$\hat{x}[k] = \frac{1}{N}\sum_{n=1}^{n_t} x[n] e^{-2\pi \mathrm{j}\frac{(k-1)(n-1)}{n_t}} \qquad \hat{x} = \overline{F}^T x = F^* x = \overline{F} x$$

Similarly, the spectra of a matrix such as K can be written as two multiplications:

$$\hat{K}[k,l] = \frac{1}{N}\sum_{i=1}^{n_t}\sum_{j=1}^{n_t} K[i,j] e^{-2\pi \mathrm{j}\left(\frac{(k-1)(i-1)}{n_t}+\frac{(l-1)(j-1)}{n_t}\right)}$$

Transform of the rows

$$\hat{K}[k,l] = \frac{1}{\sqrt{N}}\sum_{i=1}^{n_t}\left(\underbrace{\frac{1}{\sqrt{N}}\sum_{j=1}^{n_t} K[i,j] e^{-2\pi \mathrm{j}\frac{(k-1)(j-1)}{n_t}}}_{\hat{K}_c}\right) e^{-2\pi \mathrm{j}\frac{(k-1)(i-1)}{n_t}}$$

Transform of the columns

Since transforming over the rows= transforming over the columns of the transpose

$$\hat{K} = \hat{K}_c F^* = F^* K \overline{F} = \overline{F} K \overline{F}$$

von KARMAN INSTITUTE
FOR FLUID DYNAMICS

Filtering and Eigenvector’s Spectra

Introducing the eigenvalue decomposition

$$K = \sum_{r=1}^{n_t} \lambda_r \psi_r \psi_r^T = \Psi \Lambda \Psi^T$$

$$\hat{K} = F^H K \overline{F} = (F^H \Psi)\,\Lambda\,(\Psi^T \overline{F}) = \hat{\Psi}\,\Lambda\,\hat{\Psi}^T$$

Key observation

The Fourier spectrum of the correlation matrix is symmetric and is the sum of outer products of its eigenvector's spectra.

↓

Implication:

If a filter removes a certain frequency from the spectra of K, this frequency is automatically removed from all its eigenvectors!

von KARMAN INSTITUTE FOR FLUID DYNAMICS

Perfect Separation Case

Consider the correlation spectra of the synthetic test case and the temporal evolution of its first POD mode

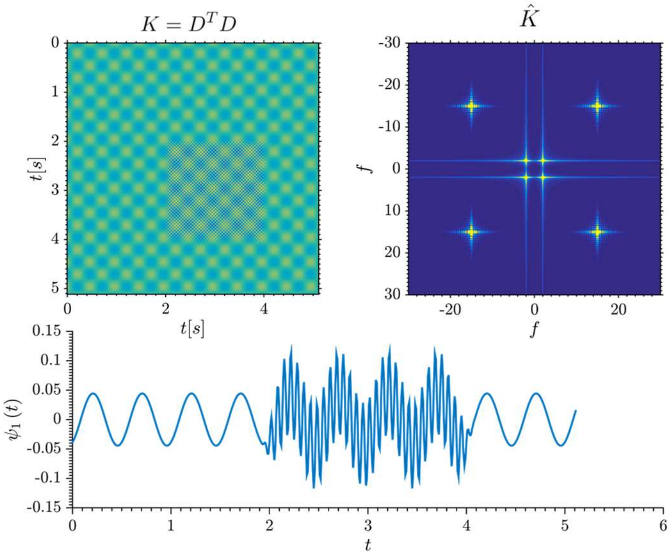

von KARMAN INSTITUTE FOR FLUID DYNAMICS

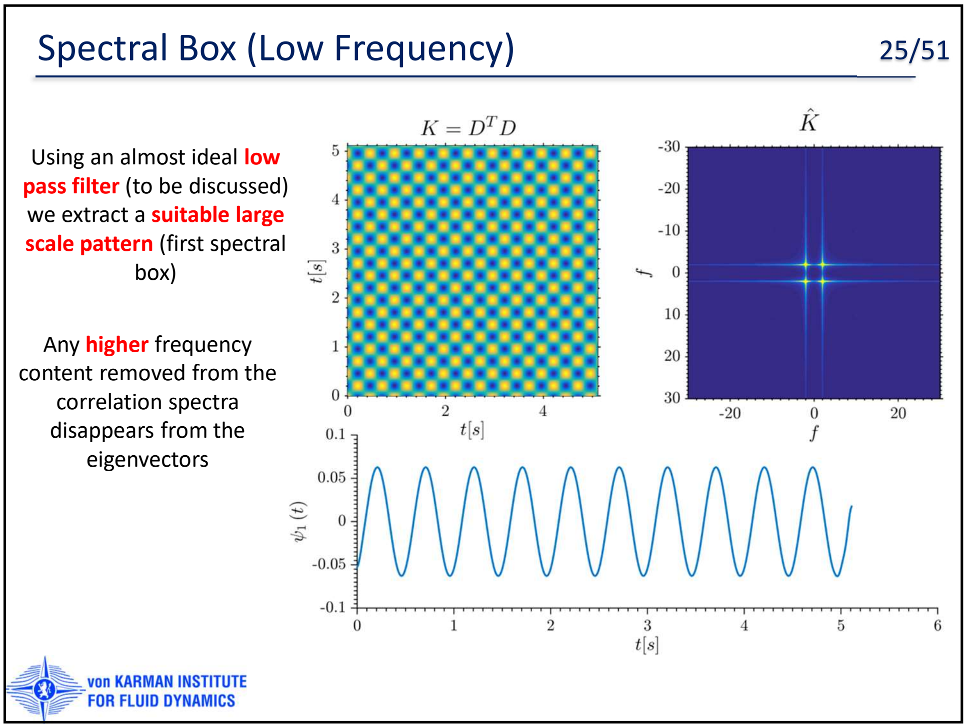

Spectral Box (Low Frequency)

Using an almost ideal **low pass filter** (to be discussed) we extract a **suitable large scale pattern** (first spectral box)

Any **higher** frequency content removed from the correlation spectra disappears from the eigenvectors

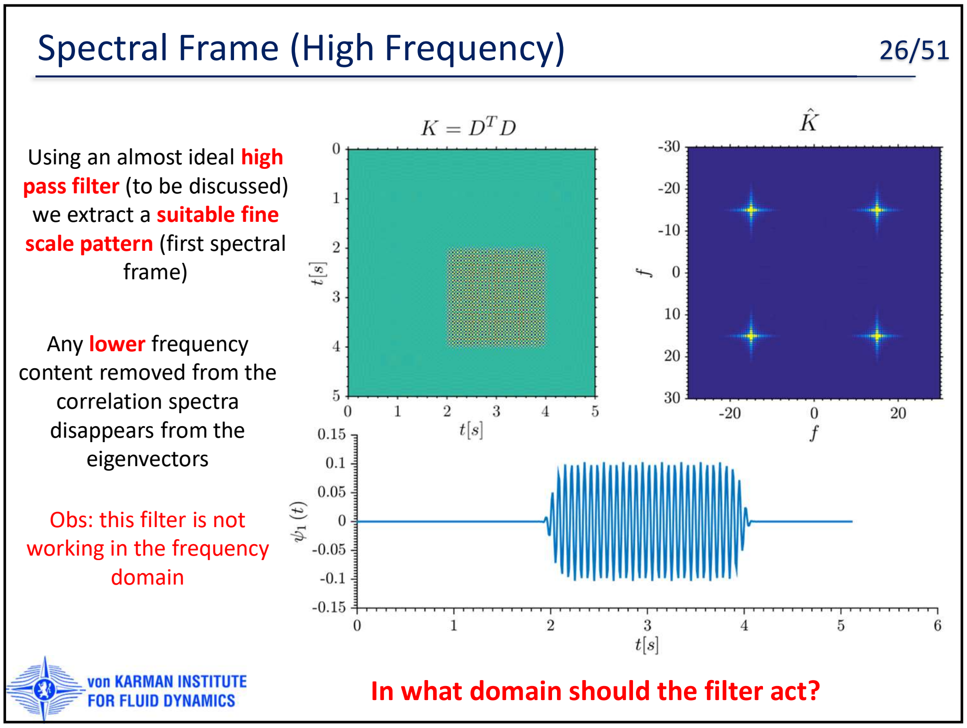

Spectral Frame (High Frequency)

Using an almost ideal **high pass filter** (to be discussed) we extract a **suitable fine scale pattern** (first spectral frame)

Any **lower** frequency content removed from the correlation spectra disappears from the eigenvectors

Obs: this filter is not working in the frequency domain

In what domain should the filter act?

Table of Contents

A Multiresolution view of K

Decompose the correlation matrix K into the contribution of different scales.

$$K = \underbrace{\overbrace{\underbrace{K_{\mathcal{L}_0}+K_{\mathcal{H}_0}}_{K_{\mathcal{L}_1}}+K_{\mathcal{H}_1}}^{K_{\mathcal{L}_2}}+K_{\mathcal{H}_2}}_{K_{\mathcal{L}_3}}+\cdots = K_{\mathcal{L}_0}+\sum_{l=0}^{l_M} K_{\mathcal{H}_l}$$

Each scale is equipped with its own POD, to be reassembled based on energy criteria

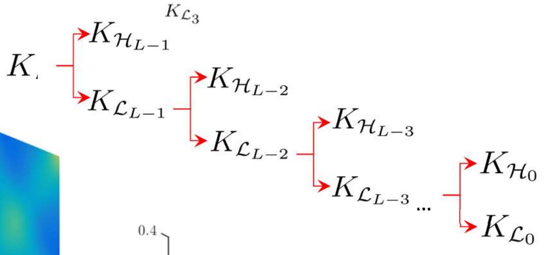

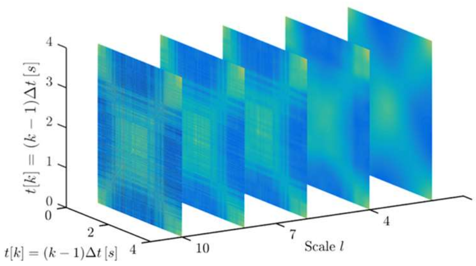

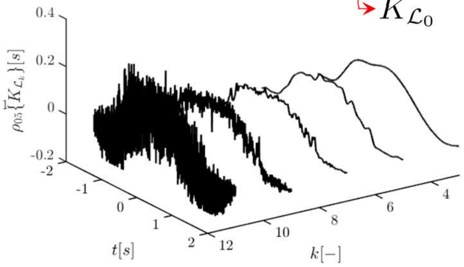

Mendez et al, Exp Therm Fluid Sci 2017

von KARMAN INSTITUTE FOR FLUID DYNAMICS

Fundamentals of 2D DWT

The correlation matrix at each scale is obtained as a linear combination of shifted basis elements called scaling functions, placed at non overlapping locations. The possible shifts depends on the scale. The approximation terms, for instance, read

Possible shifts at scale l Scaling Coefficients Scaling functions

$$K_{\mathcal{L}_l}[i,j] = \frac{1}{n_t} \sum_{m=0}^{\boxed{2^l-1}} \sum_{n=0}^{\boxed{2^l-1}} \underline{C_{s,l}[m,n]}\,\underline{s_{l,m,n}[i,j]}$$

For the last three scales, for instance, the scale functions are placed as follow

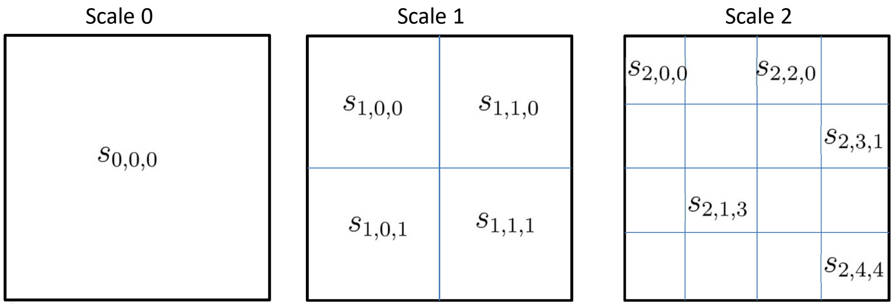

Fundamentals of 2D DWT

The reasoning for the fine scale part (detail) is analogous, expect that it contains three sets of basis elements called wavelets, on for each kind of details:

$$K_{\mathcal{H}_l}[i,j] = \frac{1}{n_t} \sum_{p}^{v,h,d} \sum_{m=0}^{2^l-1} \sum_{n=0}^{2^l-1} C^p_{w,l}[m,n] w^p_{l,m,n}[i,j]$$

The coefficients in both cases can be computed by standard projection of the matrix onto the set of bases of $m,n=[0,1,\dots 2^l-1]$ scaling or wavelet functions.

The computation of the coefficients is the Discrete Wavelet Transform (DWT);

$$C_{s,l}[m,n] = \frac{1}{n_t} \sum_{i=1}^{n_t} \sum_{j=1}^{n_t} K[i,j] s_{l,m,n}[i,j]$$

The projection of the matrix onto the coefficients is the Inverse Discrete Wavelet Transform (DWT)

$$C^p_{w,l}[m,n] = \frac{1}{n_t} \sum_{i=1}^{n_t} \sum_{j=1}^{n_t} K[i,j] w^p_{l,m,n}[i,j]$$

What are the scaling functions and the wavelet at each scale ?

2D Wavelets and Scaling Functions

At each scale, wavelet and scaling functions are synthesized by a mother function via the dilatation equation (Mallat, 1989):

$$s_{l,m,n}[i,j] = \underline{2^{l/2} s\left[2^l i - 2^{L-l} m, 2^l j - 2^{L-l} n\right]} \quad \textbf{Father Wavelet}$$

$$w^{v,h,d}_{l,m,n}[i,j] = \underline{2^{l/2} w^{v,h,d}\left[2^l i - 2^{L-l} m, 2^l j - 2^{L-l} n\right]} \quad \textbf{Mother Wavelet(s)}$$

Each of the 2D basis element is constructed as outer product of a 1D element

$$\begin{aligned} s_{k,m,n}[i,j] &= s_{k,m}[i] \otimes s_{k,n}[j] \\ w^v_{k,m,n}[i,j] &= s_{k,m}[i] \otimes w_{k,n}[j] \\ w^h_{k,m,n}[i,j] &= w_{k,m}[i] \otimes s_{k,n}[j] \\ w^d_{k,m,n}[i,j] &= w_{k,m}[i] \otimes w_{k,n}[j] \end{aligned}$$

Obs: By construction, each element in the scale (approximation or full detail) is symmetric and thus we keep the symmetry of the original matrix.

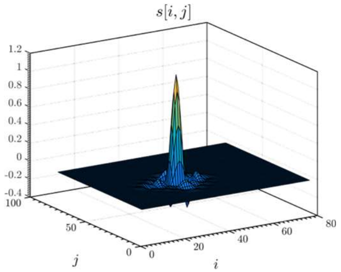

Exemplary scaling function

von KARMAN INSTITUTE FOR FLUID DYNAMICS

Table of Contents

The Final Reassembly

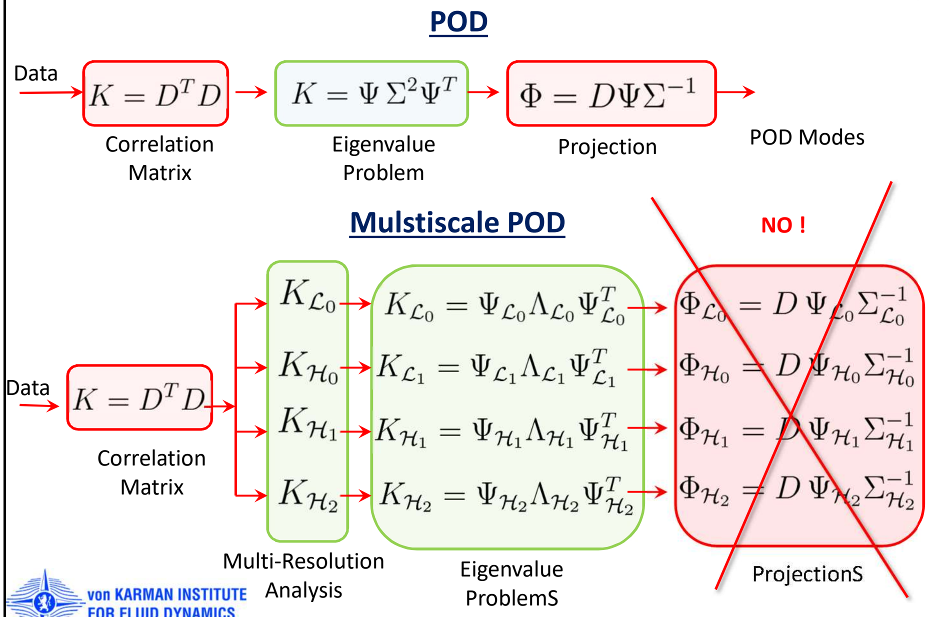

POD

Data → $K = D^T D$ → $K = \Psi\,\Sigma^2\Psi^T$ → $\Phi = D\Psi\Sigma^{-1}$ → POD Modes

Correlation Matrix

Eigenvalue Problem

Projection

Mulstiscale POD

NO !

Data → $K = D^T D$ → Correlation Matrix

$K_{\mathcal{L}_0}$, $K_{\mathcal{H}_0}$, $K_{\mathcal{H}_1}$, $K_{\mathcal{H}_2}$

$$K_{\mathcal{L}_0} = \Psi_{\mathcal{L}_0}\Lambda_{\mathcal{L}_0}\Psi^T_{\mathcal{L}_0}$$
$$K_{\mathcal{L}_1} = \Psi_{\mathcal{L}_1}\Lambda_{\mathcal{L}_1}\Psi^T_{\mathcal{L}_1}$$
$$K_{\mathcal{H}_1} = \Psi_{\mathcal{H}_1}\Lambda_{\mathcal{H}_1}\Psi^T_{\mathcal{H}_1}$$
$$K_{\mathcal{H}_2} = \Psi_{\mathcal{H}_2}\Lambda_{\mathcal{H}_2}\Psi^T_{\mathcal{H}_2}$$

$$\Phi_{\mathcal{L}_0} = D\,\Psi_{\mathcal{L}_0}\Sigma^{-1}_{\mathcal{L}_0}$$
$$\Phi_{\mathcal{H}_0} = D\,\Psi_{\mathcal{H}_0}\Sigma^{-1}_{\mathcal{H}_0}$$
$$\Phi_{\mathcal{H}_1} = D\,\Psi_{\mathcal{H}_1}\Sigma^{-1}_{\mathcal{H}_1}$$
$$\Phi_{\mathcal{H}_2} = D\,\Psi_{\mathcal{H}_2}\Sigma^{-1}_{\mathcal{H}_2}$$

Multi-Resolution Analysis

Eigenvalue ProblemS

ProjectionS

von KARMAN INSTITUTE FOR FLUID DYNAMICS

Incomplete Separation: Example

Consider the MRA decomposition of the following symmetric matrix:

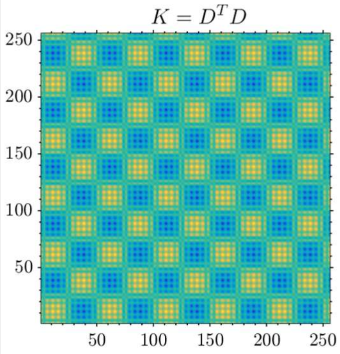

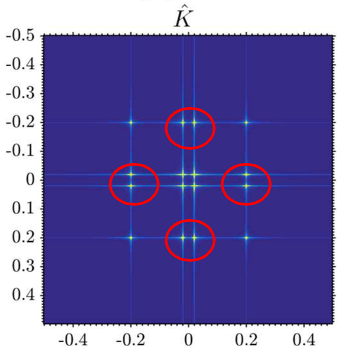

The pattern features high and low frequency content with a strong '1D' frequency

Both frequencies appear in the dominant eigenvector

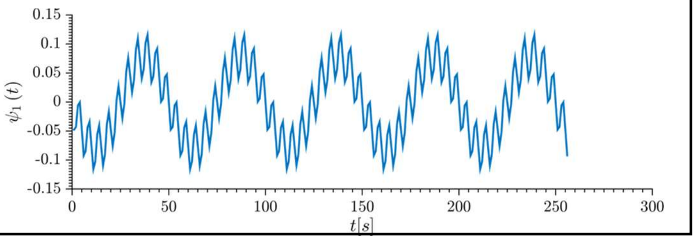

von KARMAN INSTITUTE FOR FLUID DYNAMICS

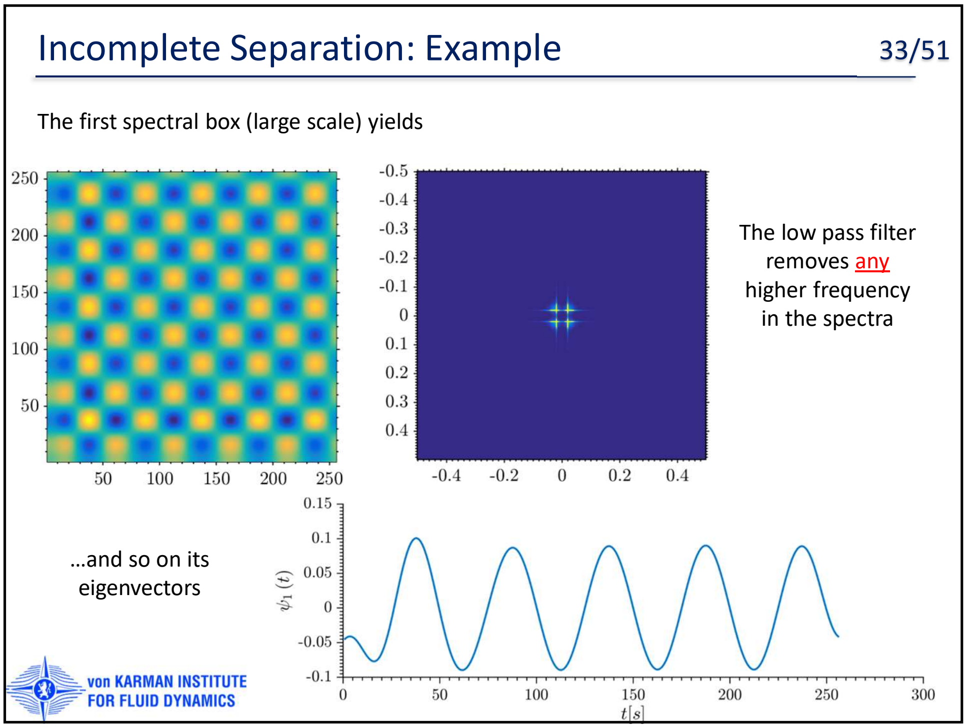

Incomplete Separation: Example

33/51

The first spectral box (large scale) yields

The low pass filter removes any higher frequency in the spectra

…and so on its eigenvectors

von KARMAN INSTITUTE FOR FLUID DYNAMICS

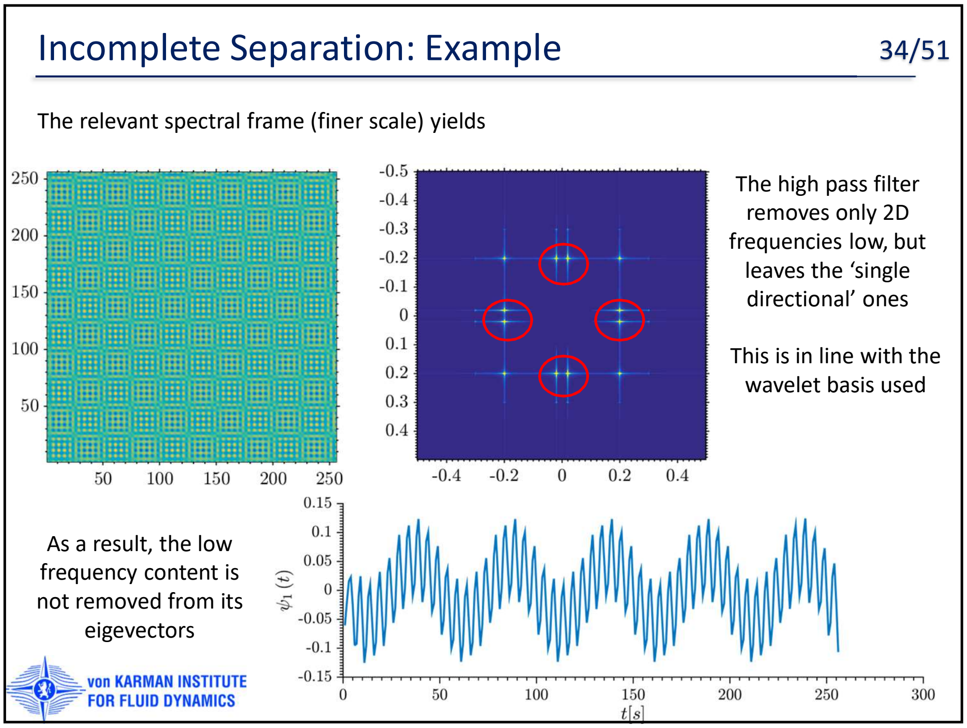

Incomplete Separation: Example

34/51

The relevant spectral frame (finer scale) yields

The high pass filter removes only 2D frequencies low, but leaves the 'single directional' ones

This is in line with the wavelet basis used

As a result, the low frequency content is not removed from its eigevectors

von KARMAN INSTITUTE FOR FLUID DYNAMICS

The Gram-Schmidt Process: Example

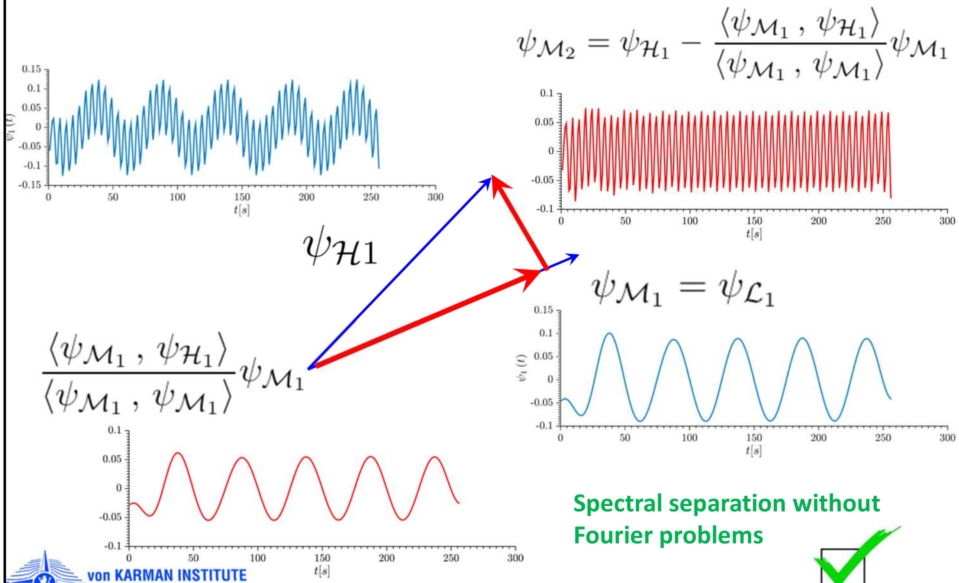

$$\psi_{\mathcal{M}_2} = \psi_{\mathcal{H}_1} - \frac{\langle \psi_{\mathcal{M}_1}, \psi_{\mathcal{H}_1} \rangle}{\langle \psi_{\mathcal{M}_1}, \psi_{\mathcal{M}_1} \rangle} \psi_{\mathcal{M}_1}$$

$$\psi_{\mathcal{H}1}$$

$$\psi_{\mathcal{M}_1} = \psi_{\mathcal{L}_1}$$

$$\frac{\langle \psi_{\mathcal{M}_1}, \psi_{\mathcal{H}_1} \rangle}{\langle \psi_{\mathcal{M}_1}, \psi_{\mathcal{M}_1} \rangle} \psi_{\mathcal{M}_1}$$

Spectral separation without Fourier problems ☑

The Final Step

Given the set of non-zero (or above tolerance) singular value at each scale

$$diag\left(\Sigma_{\mathcal{L}_m}\right) \quad diag\left(\Sigma_{\mathcal{H}_m}\right) \quad diag\left(\Sigma_{\mathcal{H}_{m-1}}\right)$$

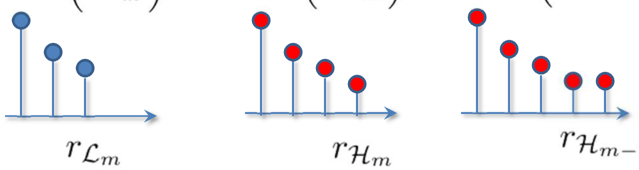

and so on…

Assembly the matrix of multiscale temporal modes starting from the large scale ones

$$\Psi^0_{\mathcal{M}} = \left[\psi_1^{\mathcal{L}_m} \dots \psi_{r_{\mathcal{L}_m}}^{\mathcal{L}_m}, \psi_1^{\mathcal{H}_m} \dots \psi_{r_{\mathcal{H}_m}}^{\mathcal{H}_m}, \psi_1^{\mathcal{H}_{m-1}} \dots \psi_{r_{\mathcal{H}_{m-1}}}^{\mathcal{H}_{m-1}}, \dots \right]$$

And re-orthonormalize to compute the temporal modes

$$\Psi^0_{\mathcal{M}} = \Psi_{\mathcal{M}}\, R \rightarrow \Psi_{\mathcal{M}} = \Psi^0_{\mathcal{M}}\, R^{-1}$$

Project and **reorder** for the spatial structures

$$D\,\Psi_{\mathcal{M}} = \Phi_{\mathcal{M}}\,\Sigma_{\mathcal{M}}$$

Table of Contents

Numerical Test Case

We consider the Vorticity-Streamline formulation of the Incompressible NS

$$\begin{cases} \omega = \nabla^2 \xi & u = \xi_y \quad , v = \xi_x \\ \omega_t = \frac{1}{Re}\nabla^2 \omega + \xi_y \omega_x - \xi_x \omega_y + \boxed{S(x,y,t)} \end{cases}$$

Solution Method (N. Kutz, 2013): Finite Differences with fast Poisson solver for the Laplacian and Runge Kutta (RK4) integration in time.

$$n_s = 256 \times 256$$

$$\mathbf{X} = (\omega, \xi)^T$$

$$\dot{\mathbf{X}} = F(\mathbf{X}, t)$$

$$\mathbf{X}(0) = \mathbf{X}_0 \longrightarrow$$

$$\begin{cases} \mathbf{X}(-L, y, t) = \mathbf{X}(L, y, t) \\ \mathbf{X}(x, -L, t) = \mathbf{X}(x, L, t) \end{cases}$$

Mendez et al, 2017
Multiscale Proper Orthogonal Decomposition (mPOD), ICNAAM

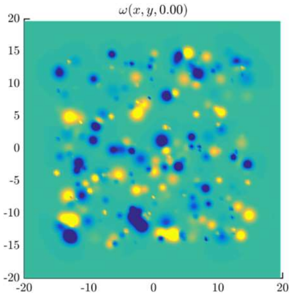

von KARMAN INSTITUTE FOR FLUID DYNAMICS

Set of Coherent Sources

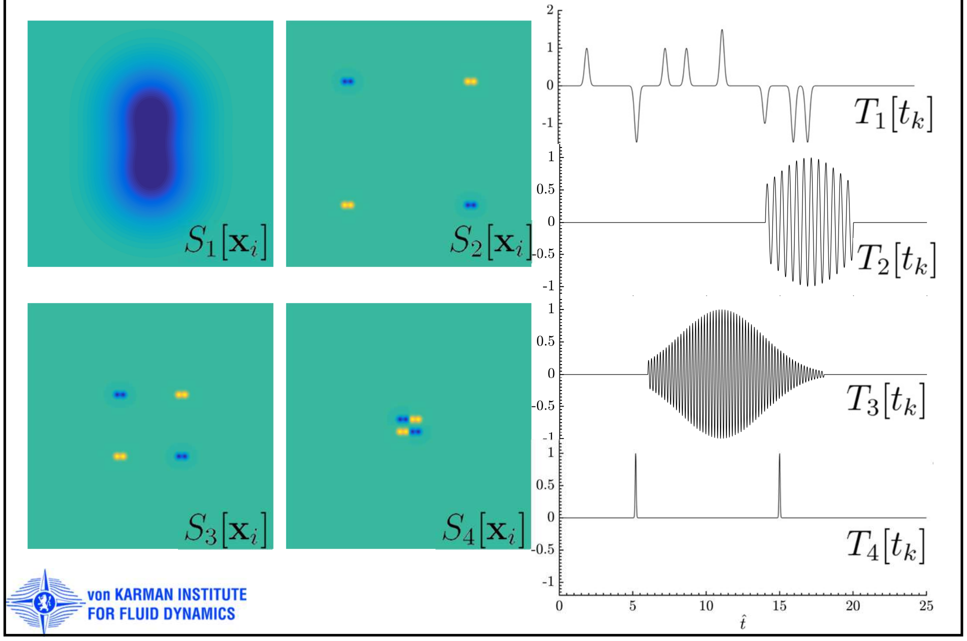

von KARMAN INSTITUTE
FOR FLUID DYNAMICS

POD Results

The correlation patter shows the footprint of different scales and events:

1) Impulsive event
2) Periodic regular pattern
3) Localization of sources
4) Strong uncorrelation

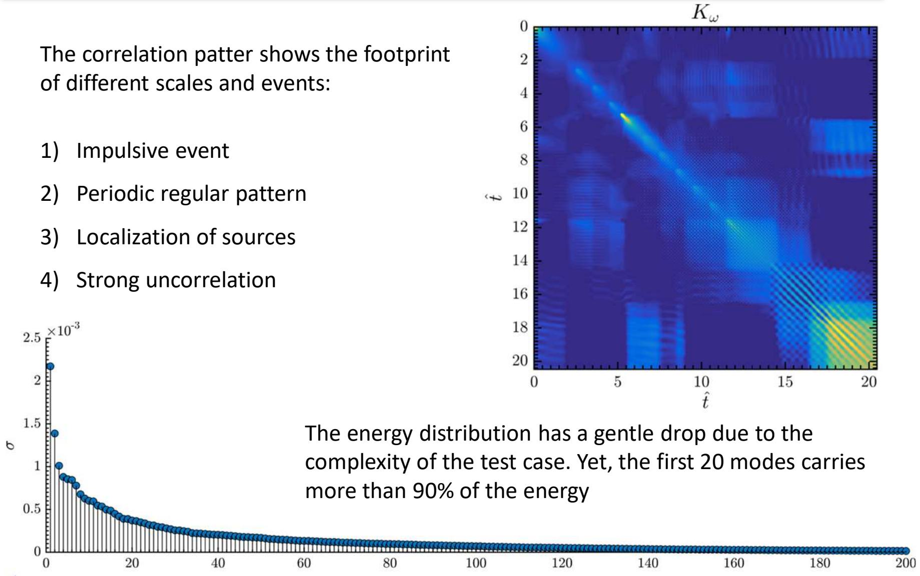

The energy distribution has a gentle drop due to the complexity of the test case. Yet, the first 20 modes carries more than 90% of the energy

von KARMAN INSTITUTE
FOR FLUID DYNAMICS

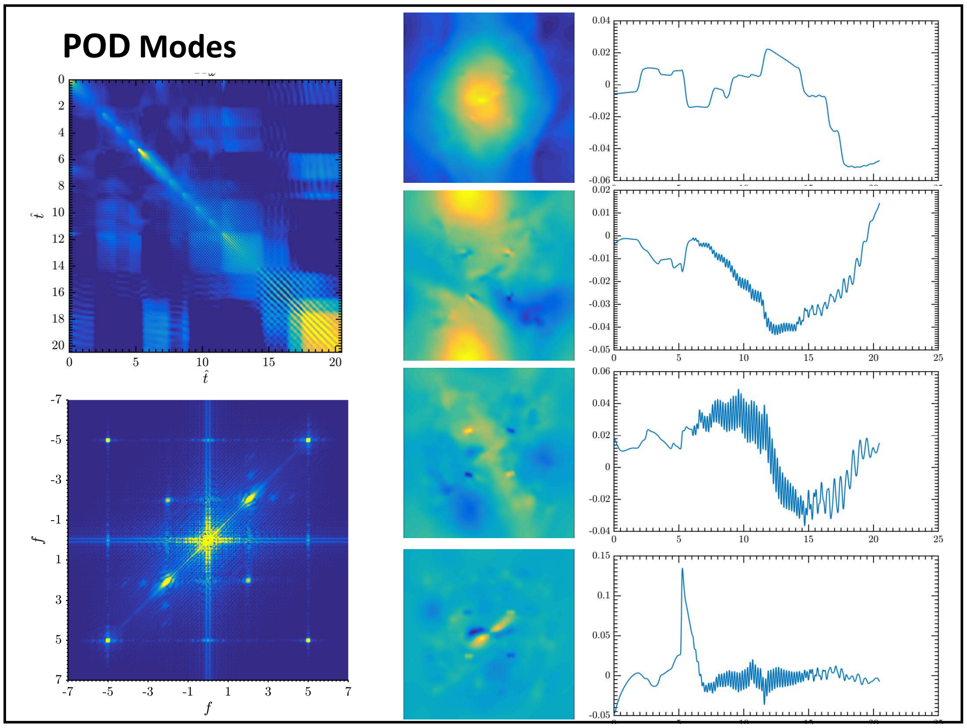

POD Modes

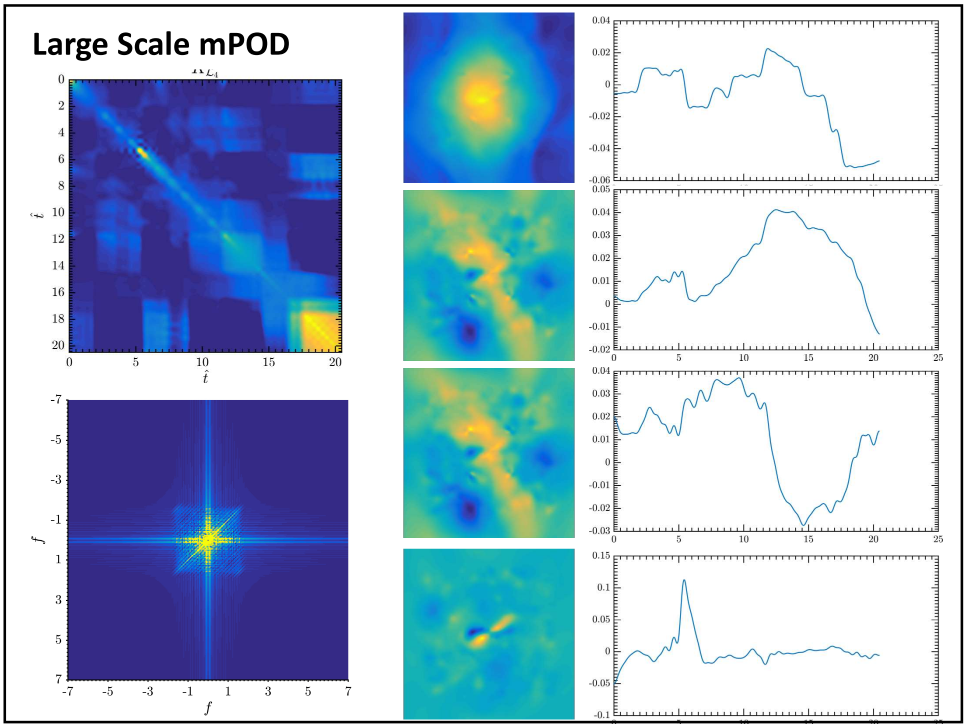

Large Scale mPOD

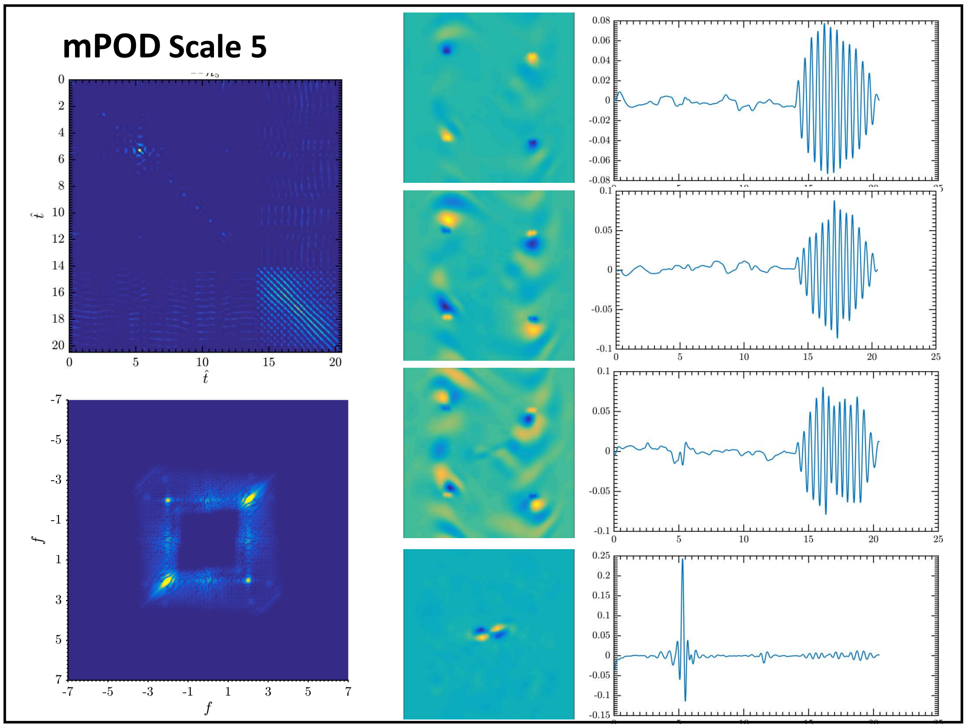

mPOD Scale 5

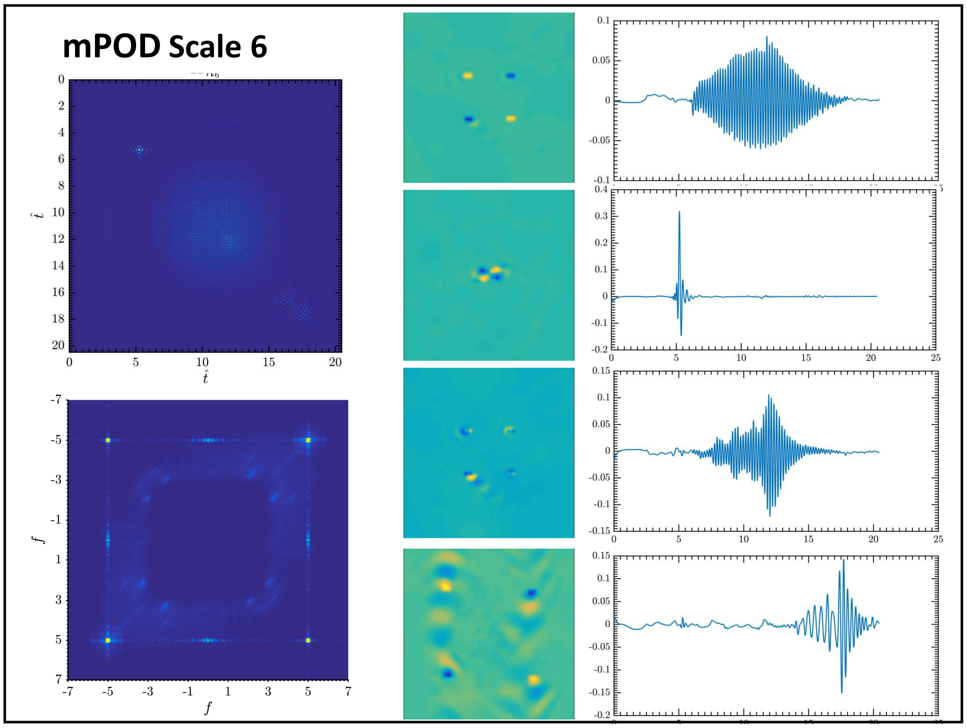

mPOD Scale 6

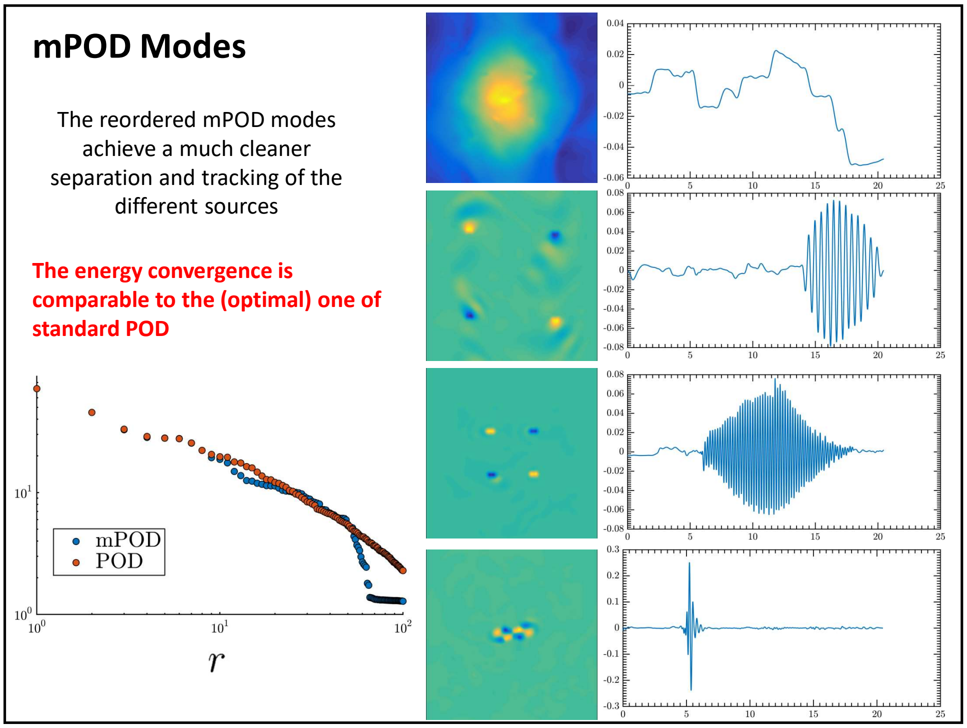

mPOD Modes

The reordered mPOD modes achieve a much cleaner separation and tracking of the different sources

The energy convergence is comparable to the (optimal) one of standard POD

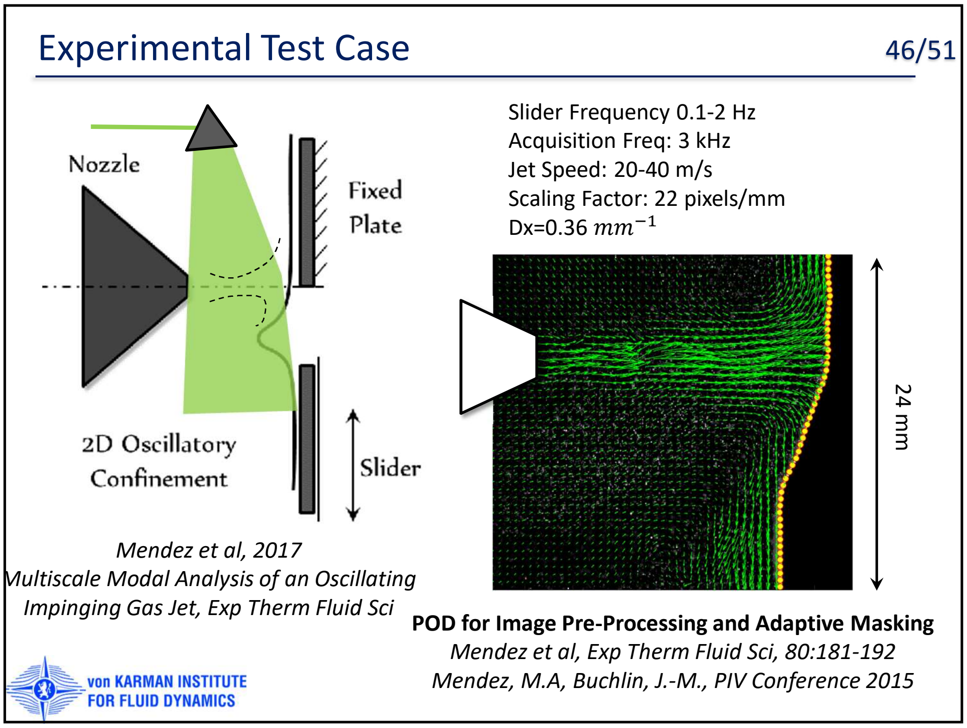

Experimental Test Case

Slider Frequency 0.1-2 Hz
Acquisition Freq: 3 kHz
Jet Speed: 20-40 m/s
Scaling Factor: 22 pixels/mm
Dx=0.36 mm^{-1}

Mendez et al, 2017
Multiscale Modal Analysis of an Oscillating Impinging Gas Jet, Exp Therm Fluid Sci

POD for Image Pre-Processing and Adaptive Masking
Mendez et al, Exp Therm Fluid Sci, 80:181-192
Mendez, M.A, Buchlin, J.-M., PIV Conference 2015

von KARMAN INSTITUTE FOR FLUID DYNAMICS

POD Modes in Quasi Steady Test

Re = 3400 (34m/s)

F=0.1 Hz

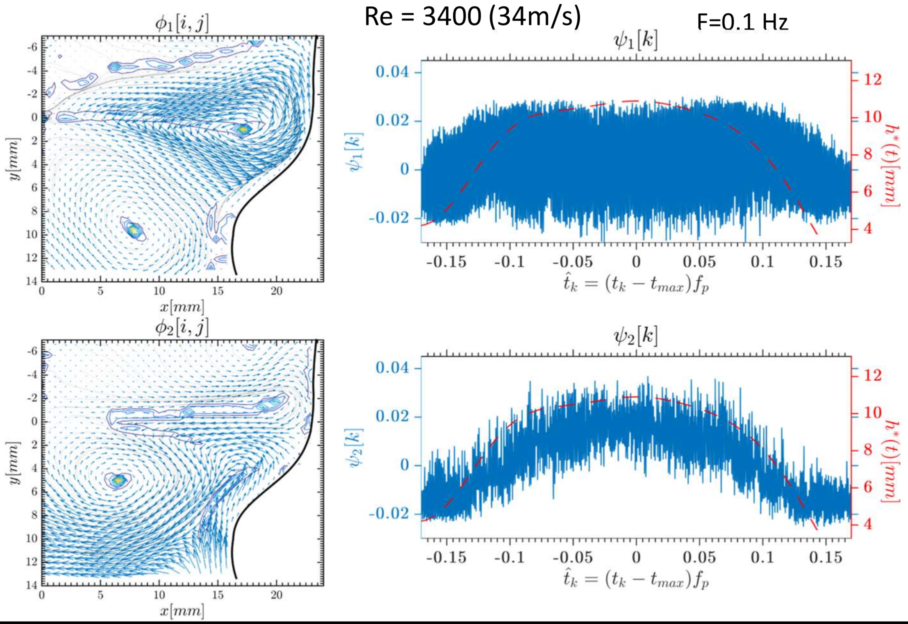

mPOD Modes in Quasi Steady Test

Re = 3400 (34m/s)

F=0.1 Hz

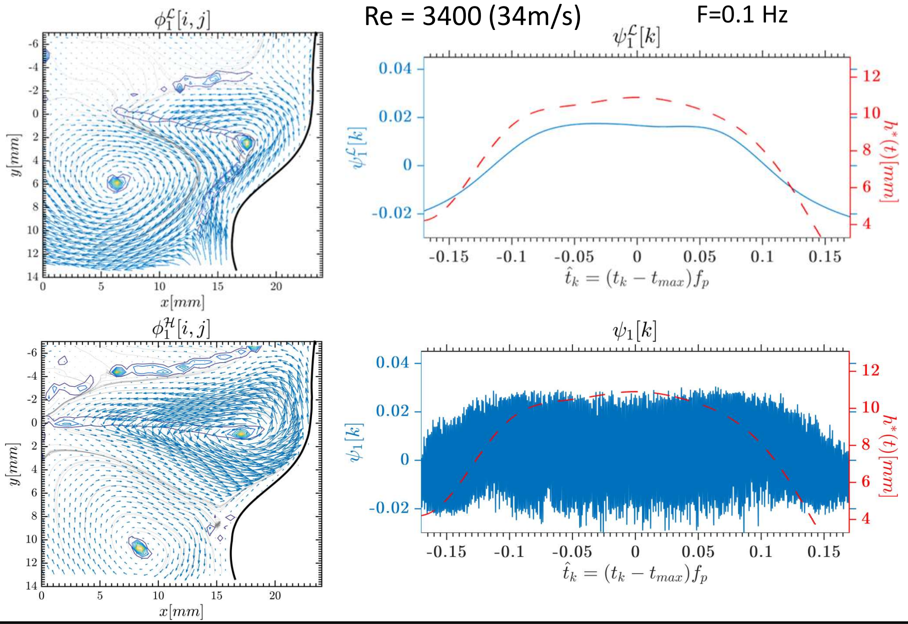

mPOD Modes Reconstruction

Two mechanisms at largely different scales are identified: the formation of a large scale vortex below the jet, which promotes a downward deflection and the flapping of the impinging jet due to entrainment unbalances

Large Scale Dynamics

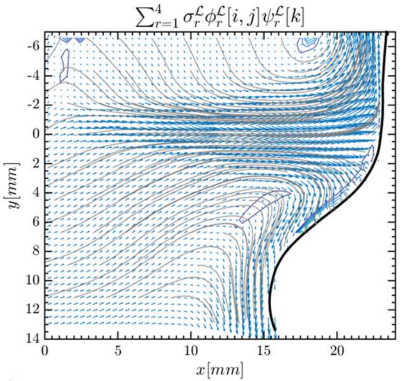

Fine Scale Dynamics

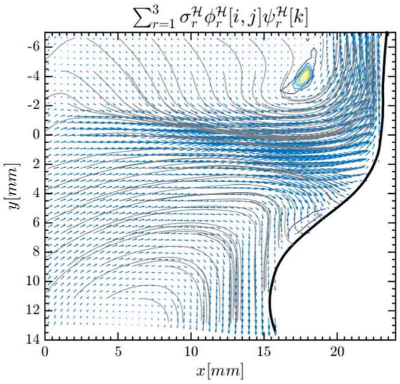

von KARMAN INSTITUTE FOR FLUID DYNAMICS

Scales Correlation

Large Scale Mode Evolution

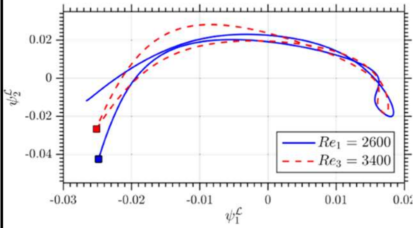

Fine Scale Versus Large Scale

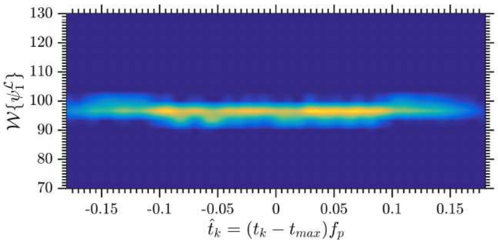

Evolution of the Energy Density in the Fluidic oscillation:

$$\mathcal{A}(\hat{t}_k) = \int_{0.9 f_h}^{1.1 f_h} \mathcal{W}\{\psi_1^{\mathcal{H}}\}(\hat{t}_k, f)df$$

versus the first large scale mode

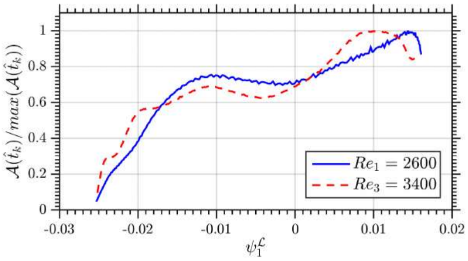

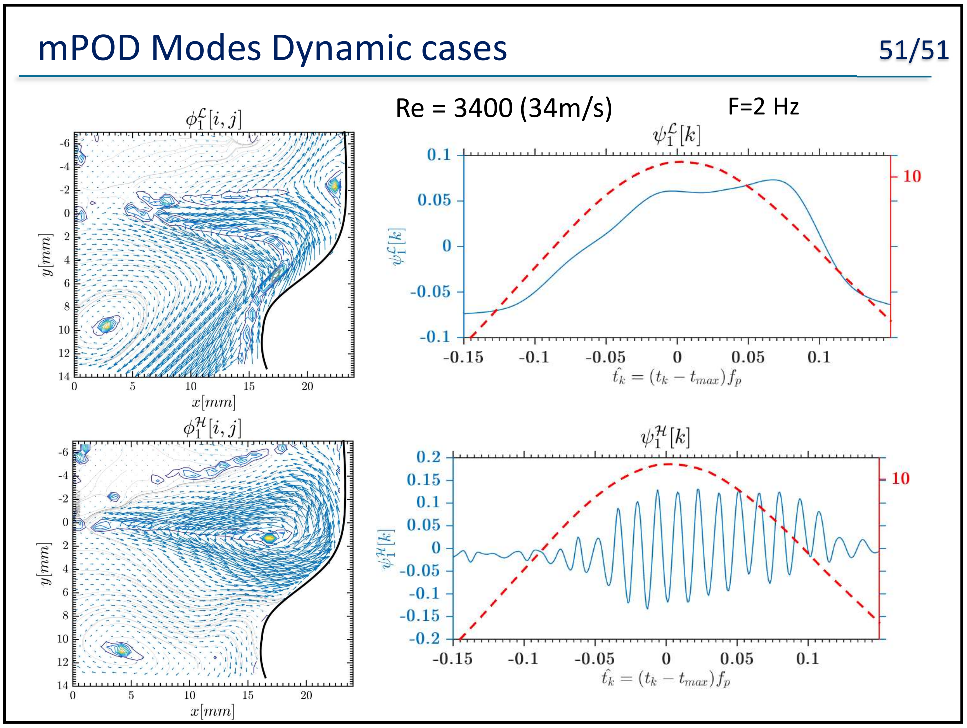

mPOD Modes Dynamic cases

Re = 3400 (34m/s)

F=2 Hz

Table of Contents

1. Motivation and Aims
2. Classification and Algebra of Decompositions
3. Synthetic Test Cases
4. The Multiscale Proper Orthogonal Decomposition
    - 3.1 Fourier Spectra and Eigenvalue Spectra
    - 3.2 Multiresolution via Discrete Wavelets
    - 3.3 The Gram-Schmidt Re-Assembly
5. Numerical and Experimental Test Cases
6. **Conclusions**

Conclusions

$$\underset{\text{Dataset}}{\underline{D\,[\mathbf{x_i},t_k]}} = \underset{\text{Information}}{\underline{D_1[\mathbf{x_i},t_k] + D_2[\mathbf{x_i},t_k]}} + \underset{\text{Something Else}}{\underline{D_3[\mathbf{x_i},t_k]\cdots + D_r[\mathbf{x_i},t_k]}}$$

$$D[\mathbf{x}_i,t_k] = \sum_{r=1}^{n_t} \sigma_r\,\phi_r[\mathbf{x}_i]\,\psi_r[t_k] = \Phi\,\Sigma\,\Psi^*$$

Energy Based: POD

Frequency Based: DFT/DMD

Mixed: SPOD

1. Classification and Algebra of Decompositions

von KARMAN INSTITUTE FOR FLUID DYNAMICS

Conclusions

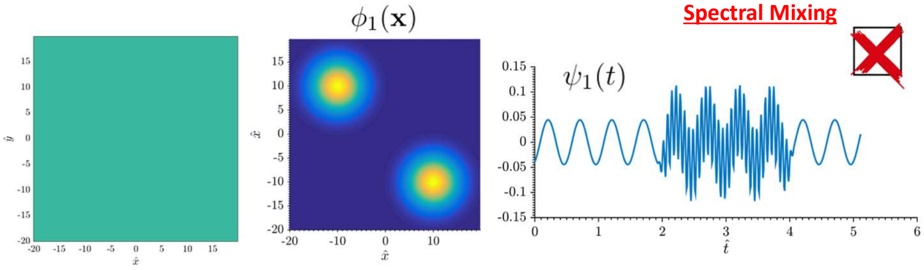

Spectral Mixing ☒

1. Classification and Algebra of Decompositions

2. Testing on Synthetic Test Cases

von KARMAN INSTITUTE FOR FLUID DYNAMICS

Conclusions

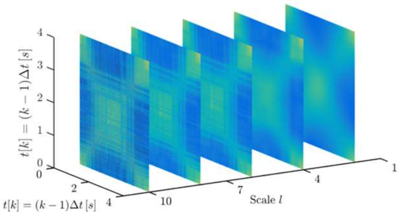

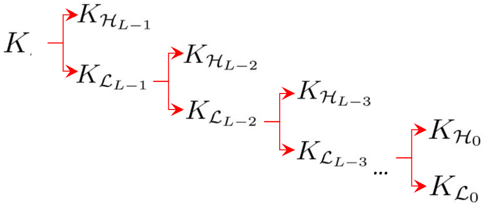

1. Classification and Algebra of Decompositions
2. Testing on Synthetic Test Cases
3. The Multiscale Proper Orthogonal Decomposition

von KARMAN INSTITUTE
FOR FLUID DYNAMICS

Conclusions

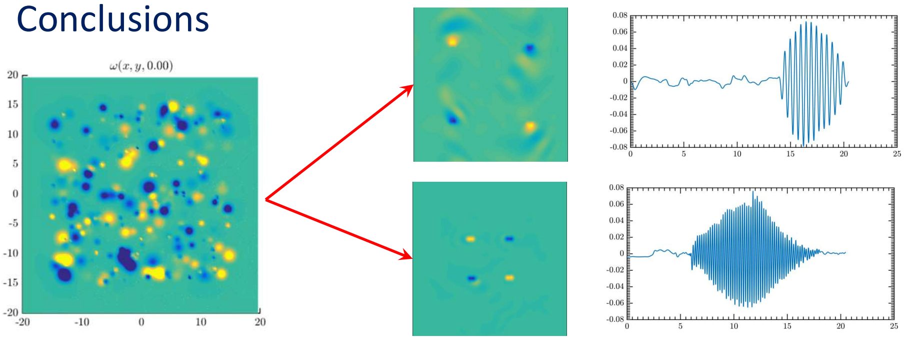

1. Classification and Algebra of Decompositions
2. Testing on Synthetic Test Cases
3. The Multiscale Proper Orthogonal Decomposition
4. Application to Numerical and Experimental Data

von KARMAN INSTITUTE
FOR FLUID DYNAMICS

Conclusions

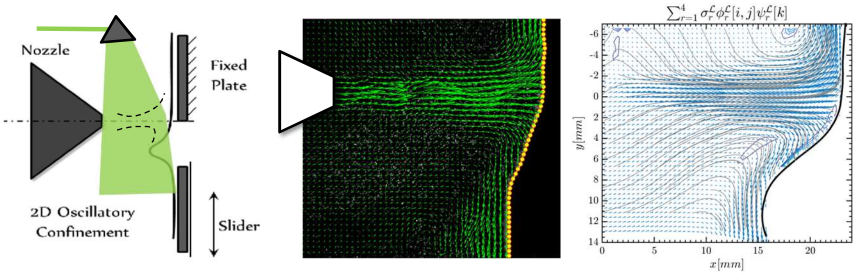

1. Classification and Algebra of Decompositions
2. Testing on Synthetic Test Cases
3. The Multiscale Proper Orthogonal Decomposition
4. Application to Numerical and Experimental Data

von KARMAN INSTITUTE
FOR FLUID DYNAMICS

Experiments in Fluid Mechanics ExFM 2017

Thank you for you Attention

von KARMAN INSTITUTE
FOR FLUID DYNAMICS

ULB UNIVERSITÉ LIBRE DE BRUXELLES